

Extracellular polymeric bacterial coverages as minimal area surfaces

Alberto Saa*

Departamento de Matemática Aplicada, IMECC - UNICAMP, 13083-859 Campinas, SP, Brazil

Omar Teschke†

Laboratório de NanoEstruturas e Interfaces, Instituto de Física - UNICAMP, 13083-970 Campinas, SP, Brazil

Surfaces formed by extracellular polymeric substances enclosing individual and some small communities of *Acidithiobacillus ferrooxidans* on plates of hydrophobic silicon and hydrophilic mica are analyzed by means of atomic force microscopy imaging. Accurate nanoscale descriptions of such coverage surfaces are obtained. The good agreement with the predictions of a rather simple but realistic theoretical model allows us to conclude that they correspond, indeed, to minimal area (constant mean curvature) surfaces enclosing a given volume associated with the encased bacteria. This is, to the best of our knowledge, the first shape characterization of the coverage formed by these biomolecules, with potential applications to the study of biofilms.

Extracellular polymeric substances (EPS) are produced by microorganisms during the process of adhesion to an environmental surface, acting mainly to protect them and to facilitate their interactions [1]. The exact functions of EPS have not been completely elucidated yet because of their extremely heterogeneous nature. It is known, however, that EPS play significant roles in the formation and function of microbial aggregates, including matrix structure formation and microbial physiological processes[2]. In this Note, we report an analysis, based experimentally on atomic force microscopy (AFM) imaging, of the EPS bacterial coverage produced in communities of *Acidithiobacillus ferrooxidans* adhered to flat plates of silicon (hydrophobic) and mica (hydrophilic). AFM has the ability to image the coverage surface morphology in aqueous conditions, without any chemical fixation. In particular, AFM has recently proved to be useful in imaging the morphology of bacteria[3], liposomes[4], and DNA molecules[5] on solid surfaces. Beech *et al.*[6], furthermore, showed that AFM allows the estimation of the width and height of bacterial exopolymeric capsule and bacterial flagella. We notice also that AFM has been recently used to characterize wetting morphologies on microstructured surfaces[7].

As we will show, AFM can be also used to determine the shape of different EPS coverage patterns of individual bacterium and some small communities of *A. ferrooxidans*. The appearance of the minimal area phenomena on extracellular polymeric coverage is associated with the need of the bacteria to prevent losing of water under drying conditions. The EPS secreted in solution or after fixation will have to cover the bacteria if they are going to survive. Since EPS production costs resources and energy to the bacteria, it would be natural to expect that EPS coverage surfaces should obey some vari-

ational principle, implying, therefore, that the observed surfaces should be *minimal* with respect to some criteria. At this scale ($\sim 1 \mu\text{m}$), on the other hand, one does not expect any other force to be relevant besides of surface tension[8, 9, 10]. Consequently, the observed surfaces should correspond to minimal area (constant mean curvature) surfaces enclosing a given and fixed volume, associated, of course, with the encased bacteria. In this way, the observed surfaces would minimize both the potential elastic energy and the total amount of EPS necessary to form them. Our analyses confirm this hypothesis, EPS coverages of *A. ferrooxidans* adhered to mica and silicon plates can be indeed understood as minimal area surfaces enclosing some fixed volumes. For a review of the biological significance of *free* (*i.e.*, without any volume constraint, zero mean curvature) minimal surfaces, see [9, 10]. Our conclusions are in agreement with the recently reported studies[7] on the minimal area surfaces associated to different wetting morphologies on microstructured surfaces.

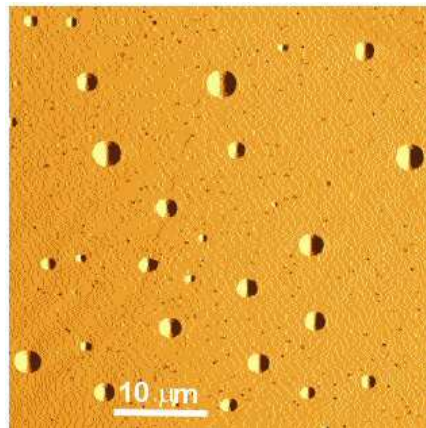


FIG. 1: *A. ferrooxidans* adhered to a hydrophilic mica plate observed in air. For all bacteria, the covering material form a cap-like structure.

EPS form a highly entangled hydrated structure, com-

*Electronic address: asaa@ime.unicamp.br

†Electronic address: oteschke@ifi.unicamp.br

posed basically by sugars and water linked by hydrogen bonds, in agreement with our optical observations suggesting that the EPS coverage behaves as a isotropic gel-like structure. Also, the typical EPS coverage has a volume 20 times larger than the encased bacterial volume. The details about the bacteria growing conditions, EPS chemical composition analysis, and the experimental setup are given in the Section Material and Methods of the Supplementary Material.

Fig. 1 shows a typical distribution of bacteria adhering to a hydrophilic mica plate at the center of the deposited droplet ($\sim 5 \text{ mL}$, 3.0 pH), corresponding to a view on an area of $\sim 2500 \mu\text{m}^2$. We notice that, typically, each bacterium is isolated from the others and the area is almost uniformly covered. The shapes of the covering structures are shown in detail in Fig. 2, where top views of individual covered bacteria are displayed; all bacteria show a cap-like structure formed by the covering material. Also, images recorded after scanning large areas provide direct evidence for the presence of a continuous layer covering part of the substrate. Although layers as thin as $\sim 20 \text{ nm}$ are observed, most of the covered substrate has thicker layers ($\sim 600 \text{ nm}$) of deposited material. We remind that bacteria shape is determined by their membranes structure, which typically have highly fluid shapes, varying from cylindrical when in a solution to some flat prolate structures when deposited on a substrate, as shown, for instance, in the dried sample depicted in Fig. 2c.

The problem of finding a minimal area surface enclosing a given volume is a classical isoperimetric (isovolume) variational problem, and several mathematical and computational tools are available to solve it in the most generic contexts. Further details of our mathematical analysis can be found in the Section Minimal Area Surfaces of the Supplementary Material. For the case of axisymmetric surfaces, analytical solutions are available, whereas for the non-symmetric case we had to use some approximations or iterative numerical methods. For the first case, one has yet two qualitative distinct cases according to the nature of the support region \mathcal{D} . For simply connected \mathcal{D} , it is well known that the minimal surface enclosing a given volume corresponds to a spherical cap. Some surfaces with multiply connected support can be well approximated by a segment of a torus. As we will see, such minimal area surfaces with multiply connected support will be useful to enlighten some of the observed structures, notably for the case of hydrophobic silicon plates.

Fig. 2 shows some observed images of the EPS coverage for single *A. ferrooxidans*. The typical surface image for the mica plates is axisymmetric and has simply connected support. Table I in the Supplementary Material shows the relevant parameters, including the observed and predicted values of the contact angle θ , for several samples in mica plates with nearly circular support \mathcal{D} . Another property of the spherical cap that can be properly checked is that its intersection with any plane must be circle arcs. Fig. 1 in the Supplementary Material

shows the χ^2 fitting of all the samples considered in Table I.

An interesting image of an axisymmetric EPS coverage surface, often observed for *A. ferrooxidans* on mica plates, is that one showed in Fig. 2(b). It consists of a spherical cap born by a thicker circular ring, which, incidentally, also has its external surface well described by a spherical segment. After rinsing these samples, one can see clearly (Fig. 2(c)) that the ring is composed by a less soluble EPS. The ring shape is very suggestive of a structure similar to the minimal toric segment (see the Supplementary Material). We notice also that such a kind of ring structure seems to be generally formed during drying processes, possibly induced by capillary flows, see [11].

For the case of hydrophobic silicon plates, the images are typically more irregular when compared with those ones observed for hydrophilic mica. This can be understood recalling that, while for a hydrophilic substrate the EPS produced by the adhered bacteria can spread over easily, occupying large areas if compared with the bacteria size, for a hydrophobic substrate the produced EPS do tend to clump and to be very sensitive to eventual surface microdefects of the substrate. Nevertheless, some of these non-symmetric coverages can be understood with the help of the axisymmetric minimal area surfaces with multiply connected support. It is the case, for instance, of the image presented in Fig. 2(d). It corresponds to a segment of a long and curved figure. Sections as that one indicated in Fig. 2(d) are nearly circle arcs, but some samples have shown up with a high degree of irregularity. The longitudinal curve is also well described by a circle arc. The question about why the coverage has such a shape has no easy answer. We foresee basically two possibilities. Such a disposition could correspond to some frustrated minimal toric segment, or maybe an initially symmetric situation, as, for instance, a section of a long prolate figure, could evolve toward the non-symmetric situation due the surface stresses induced by the microdefects of the hydrophobic substrate. The coverage surface depicted in Fig. 2(e), despite of being not exactly symmetric, is also very suggestive of a minimal toric segment. Minimal area surfaces with multiply connected support show up for the hydrophobic substrate presumably because the EPS coverage is prevented to evolve towards the globally minimal area surface (the spherical cap) due to the difficulties of spreading over the hydrophobic substrate. The EPS coverage tends, in this way, to some locally minimal area surface as, for instance, the toric segment.

The non-axisymmetric image displayed in 2(f) is a typical example of a coverage surface we had to analyze numerically. There is no analytical solution for the general non-symmetric case. However, a plenty of numerical and semi-analytical methods are available to attack this problem. These EPS coverage surfaces shall be understood as minimal area surfaces enclosing a given volume and with a given region of support \mathcal{D} . There is no hope in solv-

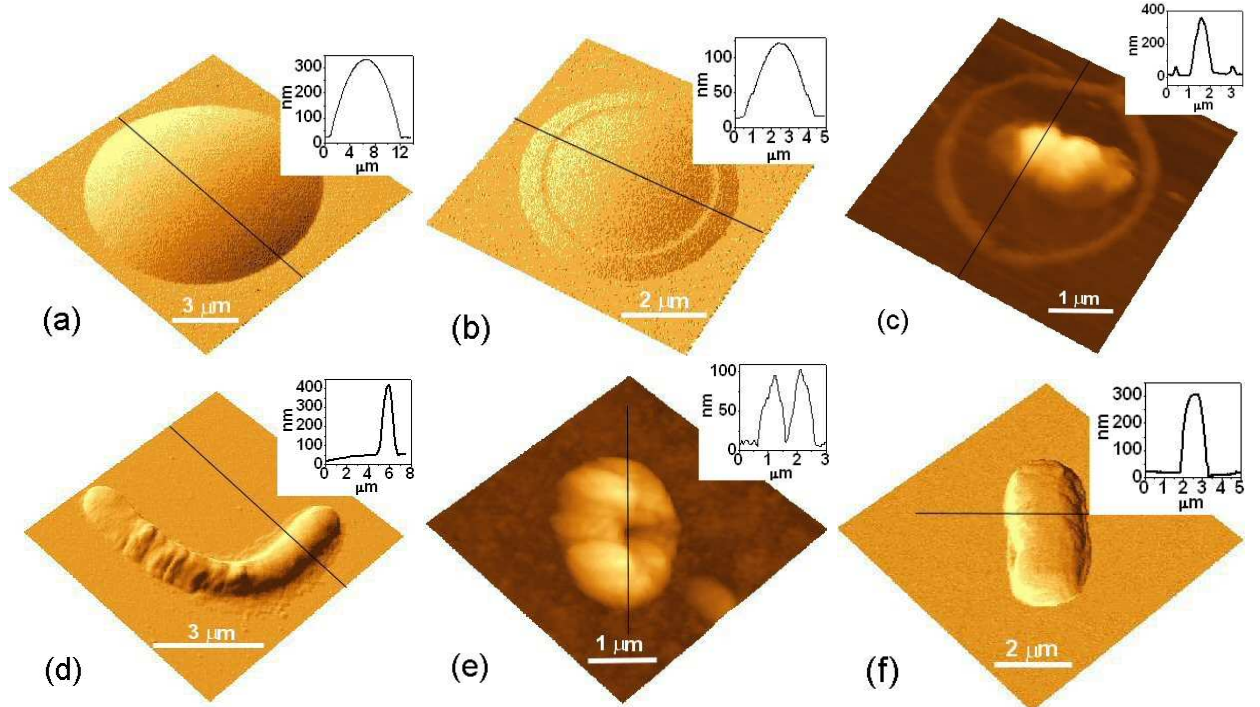


FIG. 2: Some AFM images of the EPS coverage of single *A. ferrooxidans* adhered to hydrophilic mica (a-c) and hydrophobic silicon (d-f) plates. The curves correspond to the slices indicated in the images. All images except (c) were obtained in aqueous condition. Fig. (c) corresponds to a rinsed sample similar to (b), where one can see clearly the circular ring corresponding to the thicker basis of the coverage. See the text for further details.

ing this problem analytically for generic \mathcal{D} . K. Brakke's public domain software SURFACE EVOLVER[12], nevertheless, has proved to be a powerful tool to this kind of problem. It is based on an iterative algorithm capable of find minimal area surfaces, according to quite general criteria, subjected to a given set of constraints, and for virtually any support \mathcal{D} , simply connected or not, convex or not. We have used it with success for solving our non symmetric cases. However, in these cases, due to the numerical nature of the solutions, we are basically restricted to some qualitative analysis. We have proceeded as follows. First, we find a parametric representation of the boundary $\partial\mathcal{D}$. Then, EVOLVER is ran for various volumes, until the maximal hight of the minimal area surface constrained to $\partial\mathcal{D}$ coincides with the observed coverage high. Then, a specific slice of the sample is compared with the results of EVOLVER. No χ^2 tests could be properly done in this case. However, a good agreement is observed. We notice that, by approximating the coverage 2(f) by a very long symmetric prolate surface, the central slice should correspond also to a circle arc, see Fig. 2 in the Supplementary Material.

Biofilms[1] are composed primarily of cells and EPS. Presumably, with some typical distance between the cells, their EPS coverage could touch each other without clumping together in a large and common coverage, forming a EPS mesh that will certainly conditionate the physical properties of the associated biofilm. With the cells

disposed in a quasi-regular way, such EPS mesh should resemble the periodic free minimal surfaces[9, 10]. In the same way that some important physical and biological properties of lipid-water phases, cell membranes and biopolymers are related to certain periodic free minimal surfaces (see [9, 10] for further references), one expects that relevant properties of a biofilm composed by such a EPS mesh might depend closely on the geometrical details of the EPS coverage. In this context, we notice that the complete mathematical solution of the problem of finding the minimal area surface enclosing and separating two given volumes (the double-bubble) appeared only very recently[13]. These points are still under investigation.

Acknowledgments

The authors are grateful to F.H.P. Knegt, R.F. Bergamo and L.M.M. Ottoboni for providing *A. ferrooxidans* bacteria cultures, M.E. Silva-Stenico and M.F. Fiore for the chemical quantification of carbohydrates, J. R. Castro and L. O. Bonugli for technical assistance, B.M. Longo and J. Queiroz for valuable discussions, and the funding support of FAPESP (2003/12529-4) and CNPq (523.268/1995-5).

Supplementary Material

I. MATERIAL AND METHODS

All the AFM images have been gotten by using an *A. ferrooxidans* strain LR[14] isolated from an acid effluent of the column leaching of uranium ore from Lagoa Real, BA, Brazil. The EPS composition has been analyzed according to the phenol-sulfuric acid method using glucose standard[15]. The bacterial suspension was deposited on a substrate and the total amount of sugar was determined. It was shown that the amount of sugar increased after a period of 24 hours. On the other hand, bacteria deposited in a wet (water saturated) environment did not show any presence of sugar, suggesting strongly that sugars are the main component of EPS produced by the bacteria when adhered to a substrate. Moreover, EPS produced by bacteria hold several times their weight in water[16]. EPS form, hence, a highly entangled hydrated structure, composed basically by sugars and water linked by hydrogen bonds, in perfect agreement with our optical observations suggesting that the EPS coverage behaves as a isotropic gel-like structure. We observed also that the typical EPS coverage has a volume 20 times larger than the encased bacterial volume.

The observation of samples by AFM was always preceded by a visual observation using the optical microscope attached to the AFM unit. Various areas are selected and then scanned with a large range of $\sim 50 \times 50 \mu\text{m}^2$. When regions with isolated bacterium are identified, the scanning range is lowered down until only 1 bacterium is caught. Typically 50 bacteria are observed in a large scan range image. From this, a few are selected, usually those ones with the best resolution. Considering that 15 different sample preparations were used in this work, that 5 samples were prepared from each run, and that 50 bacteria at least in each substrate were observed, the typical bacterial coverage is well represented by our images.

A. Growth conditions and sample preparation

The bacterial strain was maintained in modified TK liquid medium[17]: $\text{K}_2\text{HPO}_4 \cdot 3\text{H}_2\text{O}$, 0.4 g/L; $\text{MgSO}_4 \cdot 7\text{H}_2\text{O}$, 0.4 d/L; $(\text{NH}_4)_2\text{SO}_4$, 0.4 g/L; $\text{FeSO}_4 \cdot 7\text{H}_2\text{O}$, 33.4 g/L; where the ferrous sulfate has been included as an energy source[18]. The medium pH was adjusted to 1.8 by addition of sulfuric acid. For culture growth, an inoculum of bacteria (5% v/v) was added to 250 mL Erlenmeyers containing 100 mL of the modified TK medium. Growth was performed at 30°C under constant shaking at 150 rpm.

In order to study the topography of planktonic EPS, aliquots of liquid cultures containing 10 μL of a cell suspension that was grown to exponential phase were di-

rectly applied onto substrata. For the AFM imaging, a sample of 5 μL of cell suspension (approximately 10^9 cells/mL) was added to silicon or muscovite mica and air-dried for 2 h at 20°C in an atmosphere with 60% humidity.

B. AFM images and techniques

The model ThermoMicroscope AutoProbe CP[19] was chosen for these experiments. The tip selected had a very small radius of curvature (~ 5 nm), and the ultra-low spring constant of its cantilever (~ 0.03 N/m) allowed probing live cells to suit our objectives without damage to the biological material. Before scanning, the size and shape of the AFM probe were characterized using a titanium reference sample from ThermoMicroscope silicon grating[19]. The probe's cantilever was made of silicon nitride in a triangular shape of 200 μm in length. Contact mode topographic images were recorded, the imaging force was kept below 10 nN and the scan rate in the range of 1-4 Hz. There is no difference in the image for forward or reverse scanning. The two images may be recorded simultaneously but, since there no difference between them, usually only the forward scan is registered. Initially, we consider views of $\sim 50 \times 50 \mu\text{m}^2$ area, with the bacteria isolated from each other and randomly distributed over the substratum (*i.e.* without large void regions). A larger amplification depicts clearly coverages with a cap-like structure which can also show a tickler ring surrounding the cap; the vertical profile image shows that this structure contains a single encased bacterial cell which is shown after washing the structure with water. A single cell has the dimensions of approximately 1 μm , whereas the typical diameter of the EPS coverage is 4 μm , indicating that the ring is large enough to encircle a single bacterial cell. The images also show that most of the structure that covers bacteria cell was removed when washed with water, whereas the rings of putative insoluble material could not be removed.

The most common artifact in AFM image acquisition is the tip shape influence in the size of the images. However, the 5 nm radius tips used in this work have a negligible effect in determining the bacteria and EPS coverage profiles, which have typical size of a few micrometers. This situation was studied in [20], where we consider distortions and some other geometrical resolution limitations due to the response of conical tips of different geometries. Here, a particularly more serious drawback during AFM imaging was the tip pollution by EPS absorption. This problem was partially solved by using the above mentioned ultra-low spring cantilever. By adjusting the imaging force below 10 nN, samples could be scanned without the immersion of the tip end in the EPS layer. When a volume of EPS is attached to the tip, the result is a loss of image resolution, usually image widening or even, in some extreme cases, the fixation of the tip to the substrate and the end of the scanning action. If the

tip is dragging loose pieces of material, the results is the formation of parallel lines along the scanning direction. In any of the above cases, the scanning was interrupted and the tip changed.

II. MINIMAL AREA SURFACES

The problem[21] of finding a minimal area surface enclosing a given volume is a classical isoperimetric (iso-volume) variational problem, and several mathematical and computational tools are available to solve it in the most generic contexts. The details of our mathematical analysis will be reported elsewhere[22]. The coverage surfaces are mathematically modeled by a smooth function $f(x, y) \geq 0$ with support restricted to a region \mathcal{D} , simply connected or not, of the plane (x, y) . For the case of axisymmetric surfaces, analytical solutions are available, whereas for the non-symmetric case we had to use some approximations or iterative numerical methods. For the first case, by introducing appropriate polar coordinates (ρ, θ) , one has yet two qualitative distinct cases according to the nature of the support region \mathcal{D} . For simply connected \mathcal{D} , the minimal surface enclosing a given volume corresponds to a spherical cap with equation

$$(f(\rho) - d)^2 + \rho^2 = r^2, \quad (1)$$

where d and r are free parameters. The volume of the associated spherical cap is given by $V_0 = \frac{2\pi}{3} (r^3 - d^3) + \pi d(r^2 - d^2)$, and $\rho_{\max}^2 = r^2 - d^2$. Hence, ρ_{\max} and V_0 would be enough to determine unambiguous the surface. However, it is not an easy task to infer the volume enclosed by the surface from our AFM images, it is more convenient, instead, to use maximal high of the surface $f(0) = r + d$ or the contact angle θ between the plate and the surface at the boundary $\partial\mathcal{D}$. These quantities obey

$$\frac{2}{\tan \theta} = \frac{\rho_{\max}}{f(0)} - \frac{f(0)}{\rho_{\max}}. \quad (2)$$

The relation (2) can be verified (and it could be falsified) easily from our axisymmetric images with simply connected \mathcal{D} . The spherical cap is the global minimum of the problem, *i.e.*, if no other constraint is imposed, the minimal area surface enclosing a given volume is the spherical cap.

The second axisymmetric case corresponds to the surfaces with multiply connected support. The minimal area surface in this case is given by

$$f(\rho) - d = \int_{\rho_{\min}}^{\rho} \frac{\frac{\lambda}{2} s^2 - c}{\sqrt{s^2 - (\frac{\lambda}{2} s^2 - c)^2}} ds, \quad (3)$$

with $\rho_{\min} = (\sqrt{1 + 2\lambda c} - 1)/\lambda$, where d , λ and c are free parameters. Eq. (3) can be expressed in a closed, but rather cumbersome, form by means of elliptic functions. A very interesting case occurs for $c \gg 1/\lambda$. In such a

case, by introducing the new variable $s = \tau + \sqrt{2c/\lambda}$, $\tau \in [-1/\lambda, 1/\lambda]$, Eq. (3) can be accurately approximated by

$$f(\sqrt{2c/\lambda} + \tau) - d \approx \int_{-\frac{1}{\lambda}}^{\tau} \frac{t}{\sqrt{\frac{1}{\lambda^2} - t^2}} dt = \sqrt{\frac{1}{\lambda^2} - \tau^2} \quad (4)$$

Eq. (4) is easily recognized as the equation for a segment of a torus with radii $\sqrt{2c/\lambda}$ and $1/\lambda$. As it has been mentioned, such minimal area surfaces with multiply connected support are useful to enlighten some of the observed structures, notably for the case of hydrophobic silicon plates.

Sample	ρ_{\max} (μm)	$f(0)$ (nm)	θ_{calc} (rad)	θ_{obs} (rad)	$-d$ (μm)	r (μm)	χ^2 (10^{-4})
a (43)	3.497	193	0.110	0.09	30.699	31.015	2.1
b (158)	5.158	262	0.107	0.10	51.452	51.868	3.5
c (118)	2.345	207	0.171	0.15	12.836	13.203	6.0
d (124)	1.379	67	0.097	0.09	14.206	14.322	1.0

TABLE I: The relevant parameters, including the observed and calculated contact angles for some samples of EPS axisymmetric coverage on a mica plate. The values of d , r , and χ^2 corresponds to the χ^2 fitting of the spherical cap (Eqs. (1) and (2)). Between parenthesis, in the first column, we have the number of points read by AFM for each sample.

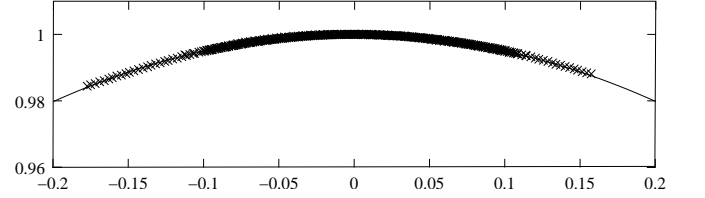


FIG. 3: For illustrative purposes, all the 543 points of the samples considered in Table I are plotted on the unitary circle defined by $x^2/r^2 + (y - d)^2/r^2 = 1$ (the solid line), where the values of d and r for each sample correspond to the χ^2 fitting of Table I. The concordance is remarkable.

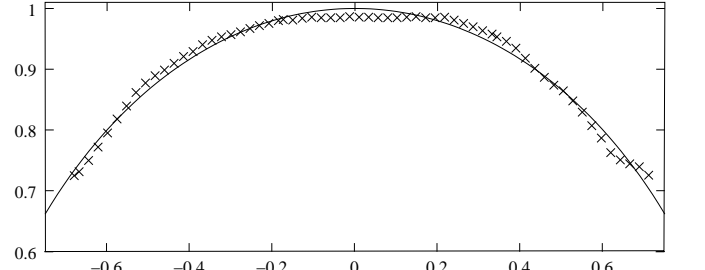


FIG. 4: The χ^2 fitting of the circle arc $x^2/r^2 + (y - d)^2/r^2 = 1$ (the solid line) for the transversal slice indicated in Fig. 2(f) of the text. The fitting corresponds to $r = 1.043 \mu\text{m}$ and $-d = 0.725 \mu\text{m}$. Circular transversal sections are good approximations for long symmetric prolate figures.

[1] L.V. Evans, *Biofilms: recent advances in their study and control*, Harwood Academic Publishers (2000).

[2] B.E. Christensen, *J. Biotechnol.* **10**, 181 (1989); T.R. Neu, and K.C. Marshall, *Biofouling* **3**, 101 (1991); T.R. Neu, *Microbiol. Rev.* **6**, 151 (1996); C.M. Buswell, *et al.*, *J. Appl. Microbiol.* **83**, 477 (1997); S. Burdman, *et al.*, *FEMS Microbiol. Lett.* **189**, 259 (2000).

[3] A. da Silva, Jr. and O. Teschke, *Bioch. et Biophys. Acta* **1643**, 95 (2003).

[4] O. Teschke and E.F. de Souza, *Langmuir* **18**, 6513 (2002).

[5] O. Teschke, R.A. Douglas, and T.A. Prolla, *Appl. Phys. Lett.* **70**, 1977 (1997).

[6] I.B. Beech, C.W.S. Cheung, D.B. Johnson, and J.R. Smith, *Biofouling* **10**, 65 (1996).

[7] R. Seemann, *et al.*, *PNAS* **102**, 1848 (2005).

[8] A.W. Adamson, *Physical Chemistry of Surfaces*, John Wiley Sons, Inc. (1990).

[9] S. Hyde, *et al.* *The Language of Shape*, Elsevier Science B.V. (1997).

[10] S. Andersson, S.T. Hyde, K. Larsson, and S. Lidin, *Chem. Rev.* **88**, 221 (1988).

[11] R.D. Deegan, *et al.*, *Nature* **389**, 827 (1997).

[12] K. Brakke, *Exper. Math.* **1**, 141 (1992); software (v2.24) available on-line at <http://www.susqu.edu/brakke/>

[13] M. Hutchings, F. Morgan, M. Ritore, and A. Ros, *Ann. Math.* **155**, 459 (2002).

[14] O. Garcia, Jr., *Rev. Microbiol.* **22**, 1 (1991).

[15] M. Dubois, *et al.*, *Analyt. Chemistry* **28**, 350 (1956).

[16] E.B. Roberson, M.K. Firestone, *Appl. Environ. Microb.* **58**, 1284 (1992); O. Teschke, *Micr. Res. Tech.* **67**, 312 (2005).

[17] O.H. Tuovinen, and D.P. Kelly, *Archiv fur Mikrobiologie* **88**, 285 (1973).

[18] R.F. Bergamo, *et al.*, *Res. in Microb.* **155**, 559 (2004).

[19] Veeco Instruments Inc., Woodbury, NY.

[20] R.M. Sasaki, R.A. Douglas, M.U. Kleinke, and O. Teschke, *J. Vac. Sci. Technol.* **B14**, 2432 (1996).

[21] L.E. Elsgolts, *Differential equations and the calculus of variations*, Mir Publishers (1970).

[22] A. Saa and O. Teschke, *Mathematical characterization of the bacterial coverage surfaces formed by extracellular polymeric substances*, to appear.